

# A Study on Melt Grafting of *N*-Halamine Moieties onto Polyethylene and Their Antibacterial Activities

Mohammad Reza Badrossamay<sup>†</sup> and Gang Sun\*

Fiber and Polymer Science, University of California, Davis, California 95616

Received October 9, 2008; Revised Manuscript Received February 2, 2009

**ABSTRACT:** Radical melt graft polymerizations of low-density polyethylene (PE) during reactive extrusion were investigated. In the absence of any reactive monomer, effects of peroxide initiator concentration and type, reaction temperature, and rotor speed of reactive extrusion on the polymer reactions were studied by monitoring mixing torque, and proper reaction conditions for the grafting reaction were proposed. Afterward, radical melt graft polymerizations of PE with several amide monomers including methacrylamide (MAM), *N*-*tert*-butylacrylamide (NTAAM), and *N*-*tert*-butylmethacrylamide (NTMAM) were continued. Fourier transform spectroscopy (FTIR) analysis and nitrogen analysis confirmed that MAM and NTAAM were successfully grafted onto PE. Monomer structures affected grafting efficiency and polymer chain combination. After exposure to chlorine bleach, the graft modified products exhibited powerful antibacterial properties against *Escherichia coli* and *Staphylococcus aureus*.

## Introduction

Functional modifications of polyolefins by using graft polymerization reactions have been of great interest in the past several decades. The grafting reactions can be carried out in solvent, melt, or solid state, while graft polymerization at the molten state has been the most preferred method, which is usually performed in the presence of a radical initiator and vinyl monomer in an extruder-so-called reactive extrusion. Absence of solvents, short reaction time, and continuous process are the main advantages of the reactive extrusion compared with other alternative techniques.<sup>1–3</sup>

Polyethylene (PE) is the second largest polymer among commodity polymers widely employed in medical devices, food packaging, automobiles, and many other products recently.<sup>4</sup> Functional PE particularly antibacterial PE products are currently needed for medical devices and food packaging, which are believed to reduce hospital related infection rates and improved food safety as well as extension of food shelf life.<sup>5</sup> Direct incorporation of antimicrobial agents into PE, such as blending into polymer and coating or adsorbing antimicrobial agents onto PE surfaces, is the most common process of producing antimicrobial PE.<sup>6</sup> Several antimicrobial agents such as nisin or simple antifungal agents such as propionic, benzoic, and sorbic acids (in the form of anhydride for increasing compatibility) have been added to LDPE to produce active packaging for food. These materials may have limited washing durability since they are mostly soluble in water.<sup>7,8</sup> Recently, Han and co-workers used polyamide as a coating medium to incorporate active compounds on surfaces of LDPE film.<sup>9,10</sup> The polyamide resin was dissolved in alcohol, and then various antimicrobial agents, such as sorbic acid, cymophenol, thymol, rosemary oleoresin, and *trans*-cinnamaldehyde, were added to the prepared solution. Afterward, the prepared medium was coated on LDPE film and irradiated with electron beams to increase covalent binding between the coating and the polymer film. In another effort, poly(2-*tert*-butylaminoethyl) methacrylate, PTBAEMA, a typical representative water-insoluble biocide, was blended with PE to provide moderate antimicrobial activity under long

contact time.<sup>11</sup> Low miscibility of this binary system has been improved by introducing a block copolymer which was synthesized by ATRP of TBAEMA onto poly(ethylene-*co*-butylene) (PEB) oligomer possessing a short polyolefin block miscible with LDPE and a PTBAEMA block.<sup>12</sup> Antimicrobial efficacy of these materials is limited depending on releasing rates of biocides and cannot be recharged after the biocides are consumed completely.

Recently, chemical incorporation of *N*-halamine precursor structures into polypropylene (PP) during melt extrusion was explored.<sup>13</sup> By using a reactive extrusion process and radical graft polymerization reaction, several cyclic and acyclic halamine precursor structures were successfully grafted onto PP. The chlorinated grafted polymers provided fast, durable, and rechargeable biocidal activities against bacteria and are prone to be applied in melt-blown nonwoven systems.

This article will demonstrate feasibility of direct production of antibacterial PE by using the reactive extrusion process. In this study, several acyclic *N*-halamine precursor compounds were grafted onto PE, and then the extruded products were converted to *N*-halamine structures by chlorination in diluted chlorine bleach. Relationship between structures and reactivity of these monomers toward PE macroradicals and biocidal action of the grafted products were examined. The modified PE showed great potential to be used in medical devices, active packaging, and water filters.

## Experimental Section

**Materials.** Low-density polyethylene granule was purchased from Aldrich (Sigma Aldrich). *N*-*tert*-Butylacrylamide (NTAAM) and methacrylamide (MAM) were obtained from TCI (TCI America), and *N*-*tert*-butylmethacrylamide (NTMAM) (Frinton) was used as received. Unless specified otherwise, dicumyl peroxide (DCP) was used as a primary initiator; 2,5-dimethyl-2,5-(*tert*-butylperoxy)hexane (DTBH) and 2,5-dimethyl-2,5-(*tert*-butylperoxy)hexyne (DTBHY) were only used for peroxide treatment of PE. Table 1 shows the chemical structures and half-lifetime of these peroxides which were obtained from Aldrich Chemicals Co. (Milwaukee, WI) and were used as received. Reagent grade acetone and xylene were used in the purifications.

**Sample Preparation.** Modification of PE was carried out in a 3 PC mixer on a Brabender Plasti-Corder ATR (C.W. Brabender) at 175 °C and 50 rpm for 10 min, unless otherwise mentioned. Nitrogen gas was purged above the mixing chamber to prevent

\* Corresponding author: Ph 530-752-0840; Fax 530-752-7564; e-mail gysun@ucdavis.edu.

<sup>†</sup> Present address: School of Engineering and Applied Sciences, Harvard University, Cambridge, MA 02138.

**Table 1. Chemical Structures and Half-Lifetimes of Applied Peroxides**

Code	Chemical Structure	Half-life (s)		
		155 °C	175 °C	195 °C
DCP		547	79	13.6
DTBH		720	110	25
DTBHY		2600	350	56

oxidation during reactions. The initial concentration of monomers was 150–450 ppm (mole per million parts of PE), while the peroxide was 4–12 ppm (mole per million parts of PE). All 40 g of reactants (PE, monomer, and peroxide) were dry mixed together for 5 min before their fast (<0.5 min) introduction into the preheated chamber (refer to Table 1s in the Supporting Information for formulation).

**Characterization.** The grafted samples were purified by dissolving in boiling xylene following by precipitation of soluble part in acetone. Grafted polymers were separated by filtration, washed several times with acetone, and then dried at 60 °C under vacuum to reach a constant weight. Very thin films of the purified samples were obtained by pressing 0.1–0.15 g sample between PTFE covered aluminum sheets under 0.1 MPa pressure at 180 °C for 45 s. Fourier transform infrared (FTIR) spectra were taken on a Nicolet Magna IR-6700 spectrophotometer from 4000 to 400  $\text{cm}^{-1}$  with a 0.1  $\text{cm}^{-1}$  resolution. At least two spectra were acquired per sample. The grafting degrees of all monomers were determined with nitrogen analysis of the purified samples. The grafted polymers were dried, pulverized, and analyzed for  $^{15}\text{N}$ . All  $^{15}\text{N}$  analyses were performed on a Europe Scientific Integra, a continuous flow isotope ratio mass spectrometer (IRMS) integrated with online combustion, at the University of California at Davis.

**Gel Determination.** The reacted samples were cut into small pieces and packed in a thimble and then were Soxhlet extracted in boiling xylene for 12 h. The gel content (%) was obtained by

$$\text{gel content} = \frac{\text{the mass after extraction}}{\text{the mass before extraction}} \times 100 \quad (1)$$

**Chlorination of Grafted Samples.** To convert the precursor structures to biocidal *N*-halamine efficiently, the purified-grafted samples were produced into micro-sized fibers through an immiscible blending extrusion process which was previously reported.<sup>13–15</sup> Subsequently, the grafted fibers were immersed in diluted chlorine bleach (~1500 ppm available chlorine) containing 0.05 wt % of a nonionic wetting agent, Triton TX-100 (Fisher Scientific, PA), for 90 min at room temperature. Then the fibers were washed thoroughly with excess amount of distilled water. An iodometric titration method was used to quantify the available active chlorine content of the grafted samples.<sup>13–15</sup>

**Antibacterial Assessment.** Antibacterial properties of the grafted samples were examined according to a modified American Association of Textile Chemists and Colorists (AATCC) test method 100 against Gram-negative bacterium *Escherichia coli* K-12 (*E. coli*) and Gram-positive bacterium *Staphylococcus aureus* ATCC 12200 (*S. aureus*). Viable bacterial colonies on the agar plates were counted after incubation at 37 °C for 24 h. The reduction of bacteria was calculated according to the following equation:

$$\text{reduction of bacteria (\%)} = \frac{B - A}{B} \times 100 \quad (2)$$

where *A* and *B* are the surviving cells (colony forming unit  $\text{mL}^{-1}$ ) on the agar plates corresponding to the activated grafted and ungrafted polyethylene fibers, respectively.

**Rheological Measurements.** Steady shearing flow behavior was studied with a capillary rheometer LCR 8052 (Kayness, PA 19543). The measuring temperature was 230 °C, and apparent shear rates varied from 5 to  $10^4 \text{ s}^{-1}$ . The ratio of length to diameter of the capillary die adopted in this work was 30, and the diameter of the capillary die was 1.0 mm. The samples were preheated for 3 min at the testing temperature before measuring.

## Results and Discussion

The possible pathway for radical graft copolymerization of PE is shown in Scheme 1. Free radicals formed through initiator decomposition can abstract hydrogen atoms from polymer backbone, resulting in formation of PE macroradicals. These macroradicals face two different possible paths: (a) react with monomers to form expected graft products or (b) undergo radical combination with each other to form cross-linked or branched products.

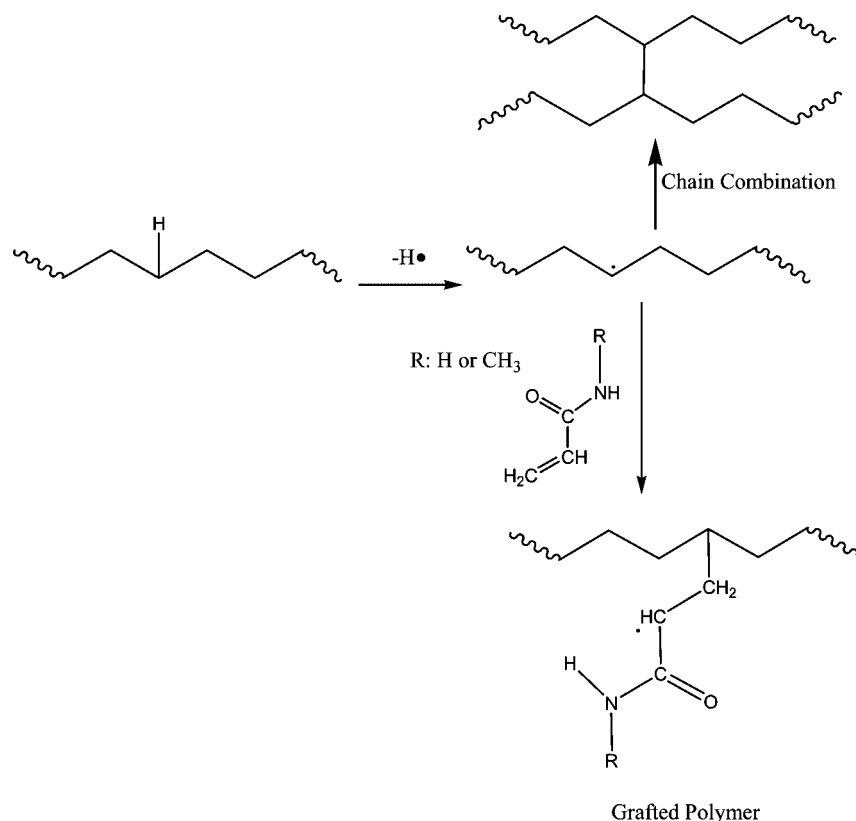
Molecular weight changes of polymers during the reactive extrusion process can be monitored by measuring torque values of the mixer during mixing since any increase in molecular weight due to cross-linking/branching will lead to higher melt viscosities and consequently higher torque values.

Since the objective of efficient grafting process was to minimize side reactions, we first decided to monitor the functions of decomposition rate, type, and content of the several commonly used peroxides on cross-linking/branching of PE in the absence of reactive monomers. Second, the optimized conditions were employed in grafting functional monomers onto PE.

**Peroxide Treatment of PE.** Peroxide treatment has been used widely to improve the mechanical and heat performance of PE.<sup>16</sup> Focuses were mainly put on final products which are cross-linked PE. As mentioned before, radical reactions of PE in the melt usually lead to a significant amount of polymer chain combination. The extent of the PE chain combination during the extrusion process could be estimated by the torque value of the system because the steady-state torque value in a batch mixer could reveal the melt viscosity, which is a function of the molecular weight of the polymer.<sup>13–15,17</sup> In Figure 1 the torque evolution of virgin PE and two DCP treated samples are shown. The torque curve kept nearly horizontal after complete melting (around 55 s) for the virgin PE, while in the case of addition of peroxides, the second peak appeared besides the melting peak. The torque decreased after passing the second peak due to an extensive scission of the partially cross-linked chains and related network. To screen polymer chain combination during the reactive extrusion, the maximum torque,  $T_{\text{max}}$ , torque ratio,  $rT = (T_{\text{max}} - T_{\text{end}})/T_{\text{end}}$  where  $T_{\text{end}}$  is the final torque, and the time location of maximum torque,  $t_{\text{loc}}$ , were evaluated. Overall,  $T_{\text{max}}$ ,  $rT$ , and  $t_{\text{loc}}$  represent amount of cross-linked chains, shear-induced scission of cross-linked structure, and time position of upper limit of cross-linking, respectively.

**Effect of Peroxide Concentration.** The effect of DCP concentration on  $T_{\text{max}}$ ,  $rT$ , and  $t_{\text{loc}}$  is shown in Table 2. By increasing the amount of DCP from 4 to 16 ppm, the  $T_{\text{max}}$  increased due to the formation of more free radicals at higher initial concentration of peroxide, which increased possibility of the chain combination. Flow curves of the peroxide treated samples show higher viscosity at low shear rate and shear thinning at high shear rate, which are typical characters of cross-linked or chain branched polymers (Supporting Information Figure 1s). However, none of the treated PE samples exhibited any cross-linking since they were all soluble in hot xylene and did not show any gel form. In addition, the Newtonian plateau at low shear rate disappeared for the high peroxide content treated samples which is another character of polymers with long chain branching. Also, there was not much difference in

Scheme 1. Overall Grafting Reaction of PE with Acyclic Halamine Precursors in Reactive Extrusion Process



$t_{loc}$  of the treated samples when the amount of DCP was increased, except at high amount of DCP. It indicates that time location of the maximum amount of the cross-linking is independent of DCP concentration. Interestingly,  $rT$  increased with increasing DCP concentration, implying that the initially formed cross-linked products may have undergone in situ degradation due to chain scission when exposed to rich free radical medium, which might be the reason that none of the samples showed any gel behavior.

**Effect of Mixing Speed.** Changing mixing speed (rotor speed) would influence the  $T_{max}$ ,  $rT$ , and  $t_{loc}$  (Table 2). By increasing the mixing speed, the maximum torque appeared at shorter times or lower  $t_{loc}$ , which implies that the radical abstracting rate was so much accelerated at more shearing rate due to higher mixing speed. Interestingly, by increasing mixing speed from 50 to 100 rpm,  $t_{loc}$  shifted from 275 to 190 s, while by decreasing to 10 rpm, the peak even did not appear sooner than 600 s. It seems that a relationship between the peak location and the rate of decomposition of the peroxide exists, which depends mainly on the reaction temperature. The efficiency of

radical-induced reaction primarily depends on the rate of peroxide diffusion into the PE phase. At a constant DCP content, the rate of DCP diffusion can likely be raised by increasing the mixing speed. Flow curves of these series of experiments validate aforementioned discussion (Supporting Information Figure 2s). The samples obtained at 10 rpm shows higher viscosity at all levels of shear rates, showing that shear degradation did not occur at low mixing rotor speed.

**Effect of Mixing Temperature.** As discussed above, if there is a correlation between the peak location and the half-lifetime of the peroxide, we would expect a shift of longer  $t_{loc}$  when reaction temperature is decreased. This is shown in Table 2. The  $t_{loc}$  was located at 150, 275, and 440 s when temperature was at 195, 175, and 155 °C, respectively. Interestingly,  $T_{max}$  was the highest at 175 °C, which could be due to thermal-induced degradation of the cross-linked/branched sample at higher temperature.

Based on the above discussions, there are several remaining questions. The first one is that the  $t_{loc}$  of the sample prepared at 10 rpm and 175 °C appeared later than 600 s instead of sooner as it was expected. The peak location and the rate of decomposition of the peroxide are all related to the half-lifetime ( $t_{1/2}$ ) of the peroxide. The longer the half-lifetime of the peroxide, the later the peak appears. Since the half-lifetime of the peroxide only depends on temperature, similar  $t_{loc}$  values were expected for samples prepared at 175 °C but under different rotor speeds. The difference in  $t_{loc}$  implies that the diffusion rate of peroxide in the PE phase plays an important role in the radical reactions of PE. Higher viscosity of molten PE system at low shear rate may be another reason, which obstructs diffusion of peroxide into PE molten phase. It is worth of noting that increasing rotor speed not only decreases viscosity of the molten phase due to shear thinning but also leads to some temperature rise due to enhanced friction, which would affect  $t_{loc}$  of the treated samples.

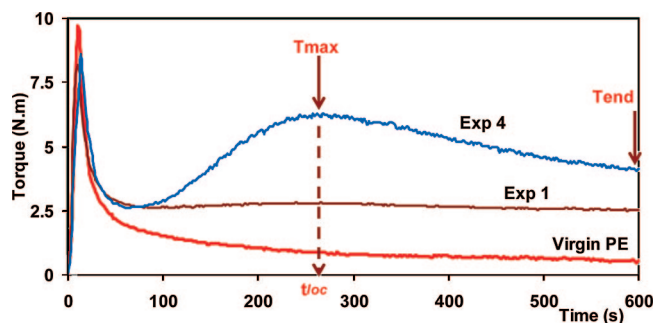


**Figure 1.** Torque evolution curves of virgin PE and peroxide treated PE, Exp 1: [DCP] = 4 ppm, 175 °C, 50 rpm; Exp 4: [DCP] = 16 ppm, 175 °C, 50 rpm.

Table 2. Composition of Peroxide-Treated Samples

	peroxide	concn (mpm)	temp (°C)	rotor speed (rpm)	$T_{\max}$ (N·m)	$rT \times 100$	$t_{loc}$ (s)
1	DCP	4	175	50	2.8	11.1	280
2	DCP	8	175	50	4.3	18.1	276
3	DCP	12	175	50	4.3	45.6	252
4	DCP	16	175	50	6.3	52.5	260
5	DCP	8	175	10	1.2	1.2	600
6	DCP	8	175	100	4.0	89.2	192
7	DCP	8	155	50	3.0	7.8	440
8	DCP	8	195	50	3.2	68.3	150
9	DTBH	8	175	50	3.9	34.0	340
10	DTBHY	8	175	50	2.6	24.8	390
11	DTBHY	8	195	50	2.91	41.3	210

The second question was about a mismatch between  $t_{loc}$  and half-lifetime of peroxide. Theoretically, more than 97% of the peroxide should be consumed after reaction time was 5 times longer than the half-lifetime of the peroxide at a particular temperature. Thus, we would expect to see the second peak around 2740, 400, and 68 s at 155, 175, and 195 °C, respectively. The results are obviously different. This mismatch is probably due to the fact that the values of the half-lifetime of the peroxides were usually measured in solvents with very low viscosities, which are quite different from the high viscous polymer in the extrusion process. In addition, aforementioned discussions validate importance of peroxide diffusion in polymers which should be accelerated at higher temperatures.

The last question is that the highest  $rT$  came from the sample prepared at 175 °C and 100 rpm, and then followed by the sample prepared at 195 °C and 50 rpm, among the all treated samples. In fact, DCP initiated macroradicals could have two simultaneously competing reactions, which are termed as chain-coupling and chain-scission mechanisms. As previously discussed, reaction temperatures and rotor speed were found to favor chain-coupling reactions (i.e., cross-linking) at the initial part of process, and then increasing them tended to make a larger contribution to chain scission.

**Effects of the Nature of Peroxide.** In addition to DCP, DTBHY and DTBH were used in the radical-induced reactions. These dialkyl peroxides are the most common initiators due to their appropriate half-lifetimes (Table 1), which will decompose to primary alkoxy radicals when heated to certain temperatures. The alkoxy radicals tend to abstract hydrogen atoms from polymer chains. The rate of radical formation is characterized by the half-lifetime of the peroxide under a temperature. As shown in Table 2, with increasing half-lifetime of the applied peroxide  $T_{\max}$  decreased. Both DTBH and DTBHY are bis-functional peroxides while DCP is not. For simplicity, at same reaction condition, we assumed DTBH and DTBHY decomposed to four primary radicals<sup>18</sup> and DCP to two primary radicals during initiation processes.<sup>1,2</sup> Then the higher  $T_{\max}$  in the case of DCP may be due to lower amount of formed primary radicals. Moreover,  $t_{loc}$  shifts to longer reaction times with increasing half-lifetime, which appeared at 290, 340, and 390 s for DCP, DTBH, and DTBHY treated samples, respectively.

In agreement with the above discussion, the  $t_{loc}$  shifts to shorter reaction times with increasing reaction temperature. In the case of DTBHY treated samples, it appears at 390 and 210 s at 175 and 195 °C, respectively.

**Peroxide-Induced Grafting of PE. FTIR Analysis.** The structures of the purified grafted samples were confirmed by FTIR spectra of the virgin PE and PE-g-NTBA and PE-g-MAM, shown in Figure 2. All the grafted samples showed characteristic peaks of PE—2850, 1460, 1370, and 720  $\text{cm}^{-1}$ —assigned to the  $\text{CH}_2$  stretching, bending deformation, and rocking deformation.<sup>19</sup> In the case of primary amide, i.e., methacrylamide grafted polyethylene (PE-g-MAM), the peak of 1660  $\text{cm}^{-1}$  due to  $\text{C}=\text{O}$

stretching (amide band I) and 1605  $\text{cm}^{-1}$  due to  $\text{N}-\text{H}$  bending (amide band II) can be observed, whereas new absorption peaks of 1660  $\text{cm}^{-1}$  (amide band I), 1550  $\text{cm}^{-1}$  (amide band II), and 3200  $\text{cm}^{-1}$  ( $\text{N}-\text{H}$  stretching of secondary amide) appeared in the case of secondary amides such as *N-tert* butylacrylamide grafted polyethylene (PE-g-NTAAM).<sup>20,21</sup> Surprisingly, there was no significant difference between spectra of virgin PE and the one which was grafted with *N-tert* butyl methacrylamide, except a small peak at 1715  $\text{cm}^{-1}$  due to  $\text{C}=\text{O}$  stretching (carboxylic acid) which may be due to polymer oxidation. It seems grafting reaction did not occur in the case of NTMAM.

**Influence of Monomer Structure on Grafting Content and Chain Combination.** Monomer structures affect the grafting content and gel content (Supporting Information Table 1s). Based on Scheme 1, the grafting reaction occurs when the macroradicals react with vinyl monomers during the extrusion process. The extent of the grafting depends mostly on reactivity of the monomer toward macroradicals. In general, the order of inherent reactivity of the radicals is approximately the inverse order of reactivity of the monomers. The most reactive monomers result in the least reactive radicals and vice versa. Polar effects, steric effects, stabilizing (resonance) effects, and thermodynamic effects are the factors that control monomer reactivity.<sup>22</sup> Thus, a substitute which decreases the reactivity of a radical would increase the reactivity of its double bond precursor. For instance, 1,1-disubstituted vinyl monomers, such as MAM, do not readily homopolymerize due to this steric hindrance.<sup>23</sup>

More steric hindered atoms in a resonance-stabilized intermediate adjacent to substituted nitrogen could further decrease the reactivity significantly. NTAAM demonstrated considerably lower reactivity toward the graft polymerization than that of MAM. Interestingly, among all these monomers, NTMAM showed the zero grafting content which may be due to existence of both the above-mentioned limits. Since the reactivity of a

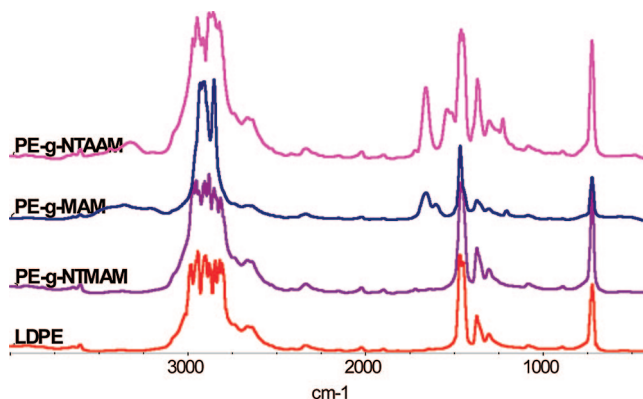
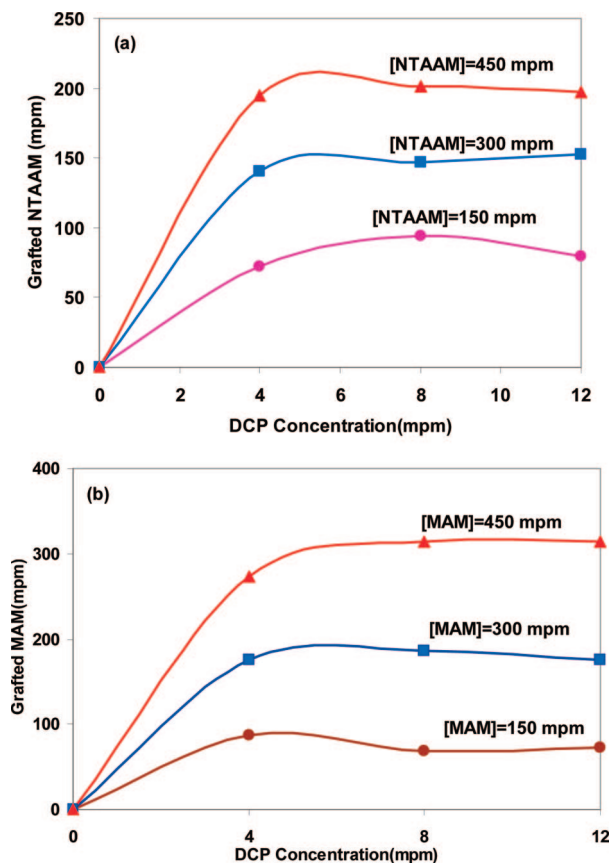


Figure 2. Spectra of virgin PE, PE-g-AAM, PE-g-NTAAM, and PE-g-NTMAM.



**Figure 3.** Influence of DCP concentration on grafting content at different monomer levels: (a) NTAAM grafted samples, (b) MAM grafted samples.

monomer toward a radical depends on the reactivities and structures of both the monomer and the radical, the bulky macroradical could obstruct accessibility of bulky monomers. Thus, larger substituents like NTMAM exhibited no grafting content.

As mentioned before, free-radical grafting of PE in the melt usually induces a significant amount of polymer chain combination. The extent of the PE chain combination during grafting process could be estimated by the torque value of the grafting system. Similar to peroxide only treated samples, the torque curve of the virgin PE was nearly horizontal after complete melting, while the torque of the PE-*g*-NTAAM sample shows a second peak after the melting peak (see Supporting Information Figures 3s and 4s). The location and intensity of these peaks are shown in the Supporting Information Table 1s. Interestingly, torque evolution curves behave in a different way in the case of PE-*g*-MAM. No detectable location or intensity of the second peaks was found (see Supporting Information Table 1s). However, there was a minimum  $T_{\max}$  with increasing the amount of the NTAAM monomer. It is intuitive that at a low content of NTAAM the peroxide dissociation leads to a formation of high concentration of PE radicals which react directly with NTAAM monomer. This reaction is inferred by cross-linking reactions. When the initial monomer content is low, the PE radicals will combine with each other, yielding a highly cross-linked structure. With increasing amount of initial monomer to 300 mpm, there would be a competition between grafting reactions and cross-linking, while the grafting reaction would be the dominant reaction. At a very high level of initial monomer, there would be formation of long-chain graft branches on polymer backbones which induced higher  $T_{\max}$ . These series of grafted samples are all soluble in hot xylene, which confirmed this explanation. The difference

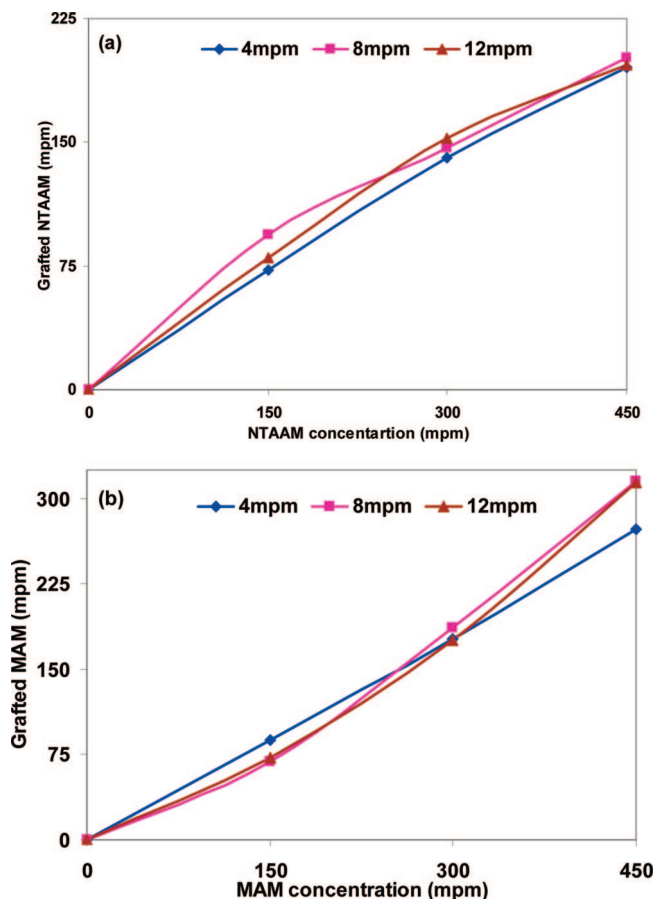
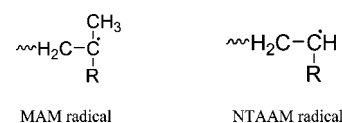


**Figure 4.** Influence of monomer concentration on grafting content at different DCP levels: (a) NTAAM grafted samples, (b) MAM grafted samples.

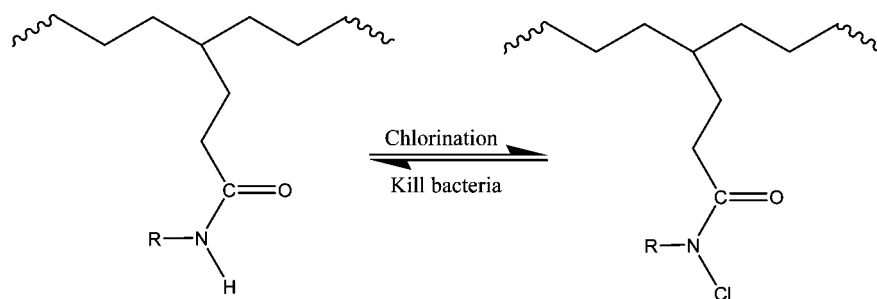
between grafting and torque evolution of MAM and NTAAM grafting systems could be explained on the stability of the tertiary MAM radical in comparison with secondary NTAAM radical:



This stability may interrupt chain combination and change torque evolution curves. Furthermore, gel content of NTAAM and MAM grafted samples did not follow the same path. For example, the gel contents in the case of MAM grafted samples overall were higher than NTAAM grafted samples and increased with increasing monomer content. It could be explained by the presence of spare methyl group in methacrylamide which may reduce the mobility of the grafted chain and promote chain combination. Further studies are needed to better understand and explain this phenomenon. By the way, the same trend was observed in the grafting of acyclic halamine precursors onto PP.<sup>24</sup>

**Influence of Initiator and Monomer Concentration.** The initial concentrations of peroxide initiator and monomer affected grafting of the monomers onto PE (Figures 3a,b and 4a,b). The initial peroxide concentration seemed to have no effect on the grafting efficiency of the monomers. The grafting content quickly reached a maximum value, and a further increase in initial peroxide concentration from 4 to 12 mpm did not improve the extent of grafting. Instead, some decrease of the grafted NTAAM content was observed at a high percentage of peroxide.

Scheme 2. Biocidal Functionality of Grafted PE



The cross-linking degree as a function of the peroxide content followed a similar way. The peroxide initiator could increase the formation of macroradicals and hence increase the chance of polymer chain combination (see the gel content in Supporting Information Table 1s). Besides, increasing peroxide concentration can promote chain transfer reactions to the monomers, which will result in either homopolymerization of the monomer and consequently reduce the concentrations of the available monomer for grafting reaction. As the initial concentration of monomers were increased from 150 to 450 ppm, regardless of the initial peroxide concentrations, the grafting contents in the case of MAM increased from about 70 to 315 ppm, under the same condition the grafting contents of NTAAM were increased from 70 to 200 ppm (Figure 3a,b). More interestingly, the grafting content is a monotonic function of the monomer concentration, which is contradictory to radical copolymerization of MAH onto PE.<sup>25</sup> In agreement with FTIR spectra, no measurable nitrogen element detected in the samples prepared with NTMAM.

**Activation.** The reaction between MAM and NTAAM and PE in the reactive extrusion was further confirmed by converting them to halamines, as illustrated in Scheme 2. Since only surface active halamine structures could demonstrate desired biocidal functions, the grafted polymers were processed into microsize fibers. After soaking in diluted chlorine bleach solutions, all fiber samples were thoroughly washed with distilled water to remove any unbounded chlorine. Virgin PE fibers did not show

any evidence of active chlorine in the titration experiments, but grafted fibers exhibited sufficient active chlorine contents (Figure 5). With an increase in the grafted monomer, the chlorine content increases in all cases but at different levels.

The primary amide monomer, such as PE-g-MAM, showed higher chlorine content than that of the secondary amide one, PE-g-NTAAM. The reason for such results may be due to either having two amide hydrogen atoms in primary amides compared with one hydrogen atom in secondary amides or less accessibility of the secondary amide hydrogen atoms due to steric hindrance of bulky pendant groups. A comparison of the grafting content and chlorine content of the resultant fibers indicates that only small percentage of the amide groups in the grafted side chains was transformed into *N*-halamines during chlorination. Such a result might be caused by the hydrophobic nature of the PE backbone which restricts the accessibility of chlorinating agents to all amide groups, and only the portion which are on the surface of the fibers were exposed to chlorine and converted to halamine structures. A similar trend has also been reported for the chlorination of *N*-halamine grafted PP fibers.<sup>13–15</sup>

In addition, pH of chlorination reaction affects the active chlorine content of the samples. Generally speaking, lower pH facilitates chlorination of amide or amine structures.<sup>14,15</sup> The active chlorine content was the lowest under alkaline bleaching condition (see Supporting Information Figure 5s). Under very mild acidic condition (pH > 5.5), in the presence of acetic acid/sodium acetate buffer, HOCl is the active species. In fact, in the presence of acetic/acetate buffer, CH<sub>3</sub>COOCl could be formed between acetic acid and chlorine, which is a more powerful chlorinating agent.<sup>26,27</sup>

**Biocidal Activity.** Biocidal properties of the chlorinated grafted fibers were examined against *S. aureus* and *E. coli* following a modified AATCC test method 100-1999, and the results are shown in Table 3. The active chlorine contents of the grafted polymers have a significant influence on the antimicrobial activity. All grafted fibers with sufficient active chlorine content provided powerful antibacterial properties against both bacteria at short contact time, even at concentration of bacteria above 10<sup>7</sup> CFU/mL.

## Conclusion

Melt graft modification of low-density polyethylene (PE) with several acyclic *N*-halamine precursors such as methacrylamide (MAM), *N*-tert-butylacrylamide (NTAAM) and *N*-tert-butylmethacrylamide (NTMAM) have been reported in this article. Different types and concentrations of peroxide initiators as well as reaction temperature and mixing speed affected polymer chain combination and grafting reactions, and reaction efficiency mainly depends on rate of diffusion of reactants into molten polymer.

The grafted PE was characterized by nitrogen analysis and FTIR instrumental analysis. Monomer structures showed significant influence on grafting content and polymer chain

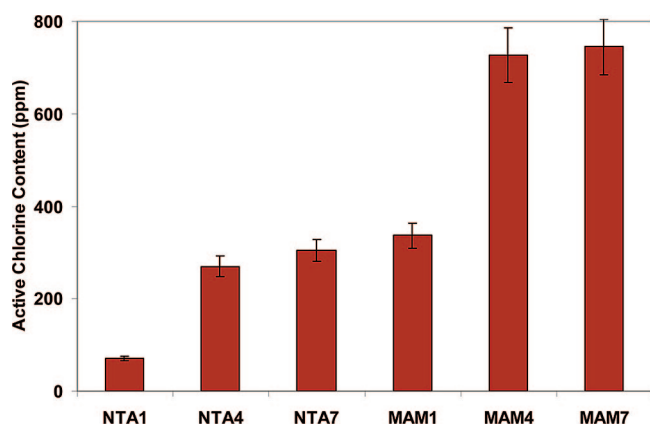


Figure 5. Active chlorine content of grafted samples (for sample composition see Table 1s) at pH = 5.5 for 90 min.

Table 3. Bacterial Reduction Percentage of the Activated Grafted Samples<sup>a</sup>

bacteria	<i>E. coli</i>	<i>S. aureus</i>
concentration	1.0 × 10 <sup>7</sup> CFU/mL	2.0 × 10 <sup>7</sup> CFU/mL
	0.5 h contact time	0.5 h contact time
MAM7	99.999	99.999
NTA7	99.9	70.0

<sup>a</sup> Active chlorine content: MAM7: 745 ppm; NTA7: 304 ppm.

combination. The presence of bulky pendant group adversely affected grafting reactions. Upon chlorine bleaching of the grafted products some of amide groups of the grafted side chains were transformed into *N*-halamines, which provided powerful antimicrobial properties against both Gram-negative and Gram-positive bacteria.

**Acknowledgment.** The authors are grateful for the financial support from the National Science Foundation (DMI 0323409 and CTS 0424716), National Textile Center (S06-CD01), and a contract from Defense Threat Reduction Agency (HDTRA1-08-1-0005).

**Supporting Information Available:** Additional information on the composition of peroxide-induced grafted samples (Table 1s) supplementary flow curves of peroxide treated samples at different DCP concentration (Figure 1s), flow curves of DCP treated samples at different rotor speed (Figure 2s), torque evolution curves of two NTAAM grafted PE (Figure 3s), torque evolution curves of two MAM grafted PE (Figure 4s), influence of DCP concentration on grafting content at different monomer levels (Figure 5s), influence of monomer concentration on grafting content at different DCP levels (Figure 6s), and effect of pH on active chlorine content of sample MAM4 (Figure 7s). This material is available free of charge via the Internet at <http://pubs.acs.org>.

## References and Notes

- (1) Moad, G. The Synthesis of Polyolefin Graft Copolymers by Reactive Extrusion. *Prog. Polym. Sci.* **1999**, *24*, 81–142.
- (2) Russell, K. E. Free Radical Graft Polymerization and Copolymerization at Higher Temperatures. *Prog. Polym. Sci.* **2002**, *27*, 1007–1038.
- (3) Hu, G. H.; Flat, J. J.; Lambla, M. In *Reactive Modifiers for Polymers*; Al-Malaika, S., Ed.; Chapman & Hall: London, 1996; p 1.
- (4) Goddard, J. M.; Hotchkiss, J. H. Polymer Surface Modification for the Attachment of Bioactive Compounds. *Prog. Polym. Sci.* **2007**, *32*, 698–725.
- (5) Brody, A. L.; Strupinsky, E. R.; Kline, L. R. *Active Packaging for Food Applications*; CRC Press: Boca Raton, FL, 2001; p 131.
- (6) Badrossamay, M. R.; Sun, G. Enhancing Hygiene Antimicrobial Properties of Polyolefins. In *Polyolefin Fibers: Industrial and Medical Applications*; Ugbole, S. C. O., Ed.; Woodhead Publishing: Cambridge, UK, 2009; p 262.
- (7) Cutter, C. N.; Willett, J. L.; Siragusa, G. R. Improved Antimicrobial Activity of Nisin-incorporated Polymer Films by Formulation Change and Addition of Food Grade Chelator. *Lett. Appl. Microbiol.* **2001**, *33*, 325–328.
- (8) Weng, Y. H.; Hotchkiss, J. H. Anhydrides as Antimycotic Agents added to Polyethylene Films for Food Packaging. *Packag. Technol. Sci.* **1993**, *6*, 123–128.
- (9) Han, J.; Castell-Perez, M. E.; Moreira, R. G. The Influence of Electron Beam Irradiation on the Effectiveness of Trans-cinnamaldehyde-coated LDPE/Polyamide Films. *J. Food Sci.* **2006**, *71*, E245–E251.
- (10) Han, J.; Castell-Perez, M. E.; Moreira, R. G. The Influence of Electron Beam Irradiation of Antimicrobial-coated LDPE/Polyamide films on Antimicrobial Activity and Film Properties. *LWT—Food Sci. Technol.* **2007**, *40*, 1545–1554.
- (11) Seyfriedsberger, G.; Rametsteiner, K.; Kern, W. Polyethylene Compounds with Antimicrobial Surface Properties. *Eur. Polym. J.* **2006**, *42*, 3383–3389.
- (12) Lenoir, S.; Pagnoulle, C.; Galleni, M.; Compère, P.; Jérôme, P.; Detrembleur, C. Polyolefin Matrixes with Permanent Antibacterial Activity: Preparation, Antibacterial Activity, and Action Mode of the Active Species. *Biomacromolecules* **2006**, *7*, 2291–2296.
- (13) Badrossamay, M. R.; Sun, G.; Durable and Rechargeable Biocidal Polypropylene Polymers and Fibers Prepared by Using Reactive Extrusion. *J. Biomed. Mater. Res., Part B*, in press.
- (14) Badrossamay, M. R.; Sun, G.; Graft Polymerization of *N*-tert-butylacrylamide onto Polypropylene During Melt Extrusion and Biocidal Properties of its Products. *Polym. Eng. Sci.*, in press.
- (15) Badrossamay, M. R.; Sun, G. Rechargeable Biocidal Polypropylene prepared by Melt Radical Grafting of Polypropylene with Diallyl-Amino Triazine. *Eur. Polym. J.* **2008**, *44*, 733–742.
- (16) Liu, M.; Yu, W.; Zhou, C. Selectivity of Shear rate on Chains in Polymer Combination Reaction. *J. Appl. Polym. Sci.* **2006**, *100*, 839–842.
- (17) Cartier, H.; Hu, G. H. Styrene-assisted Melt Free Radical Grafting of Glycidyl Methacrylate onto Polypropylene. *J. Polym. Sci., Part A: Polym. Chem.* **1998**, *36*, 1053–1063.
- (18) Tang, F.; Huyser, E. S. Thermal Decomposition of Bifunctional Peroxides. *J. Org. Chem.* **1977**, *42*, 2160–2164.
- (19) Gulmine, J. V.; Janissek, P. R.; Heise, H. M.; Akcelrud, L. Polyethylene Characterization by FTIR. *Polym. Test.* **2002**, *21*, 557–563.
- (20) Socrates, G. *Infrared and Raman Characteristic Group Frequencies: Tables and Charts*, 3rd ed.; John Wiley & Sons: London, 2004; p 143.
- (21) Kuptsov, A. H.; Zhizhin, G. N. *Handbook of Fourier Transform Raman and Infrared Spectra of Polymers*; Elsevier: Amsterdam, 1998.
- (22) Matyjaszewski, K.; Davis, T. P. *Handbook of Radical Polymerization*; Wiley-Interscience: Hoboken, 2002.
- (23) Moad, G.; Solomon, D. H. *The Chemistry of Radical Polymerization*, 2nd ed.; Elsevier: Amsterdam, 2006; p 392.
- (24) Badrossamay, M. R.; Sun, G. Acyclic Halamine Polypropylene Polymer: Effect of Monomer Structure on Grafting Efficiency, Stability and Biocidal Activities. *React. Funct. Polym.* **2008**, *68*, 1636–1645.
- (25) Lu, B.; Chung, T. C. Synthesis of Maleic Anhydride Grafted Polyethylene and Polypropylene, with Controlled Molecular Structures. *J. Polym. Sci., Part A: Polym. Chem.* **2000**, *38*, 1337–1343.
- (26) Armesto, X. L.; García, M. V.; Santaballa, J. A. Aqueous Chemistry of N-halo Compounds. *Chem. Soc. Rev.* **1998**, *27*, 453–460.
- (27) Thomm, E. W. C. W.; Wayman, M. N-Chlorination of Secondary Amides. I. Kinetics of N-Chlorination of N-methyl acetamide. *Can. J. Chem.* **1969**, *47*, 3219–3297.

MA802270B